Perturbed vacuum magnetic field and global $m = 2$ components associated with geodesic acoustic modes in tokamaks

C. Wahlberg[1] and J. P. Graves[2]

[1]*Department of Physics and Astronomy, P.O. Box 516, Uppsala University, SE-751 20 Uppsala, Sweden;* [2]*Ecole Polytechnique Fédérale de Lausanne (EPFL), Swiss Plasma Center (SPC), CH-1015 Lausanne, Switzerland.*

Introduction While the geodesic acoustic continuum mode (GAM) in tokamaks is often treated as an electrostatic phenomenon [1], recent experiments [2, 3] and theory [4, 5] have shown that a magnetic component with (dominant) poloidal mode number $m = 2$ is also associated with the mode. This feature of GAMs can be understood by using an ideal MHD description of the plasma, where the magnetic component (**Q**) of the GAM is calculated from $\mathbf{Q} = \nabla \times (\boldsymbol{\xi} \times \mathbf{B})$, and $\boldsymbol{\xi}$ is a plasma displacement perturbation with mode number $m = 2$, also associated with the GAM [4, 5]. This global $m = 2$ component of $\boldsymbol{\xi}$ exists within the whole plasma region and is driven by a combination of the effects of a finite pressure at the GAM surface and toroidal geometry. Similarly to the $m = 2$ component of $\boldsymbol{\xi}$, the magnetic perturbation also exists within the whole plasma, and even in the vacuum region, where it recently has been detected in experiments [2, 3]. The $m = 2$ component of $\boldsymbol{\xi}$ generates, in addition, fluctuations in the plasma density, also existing within the whole plasma, and in particular in regions of strong density gradients, e.g. near the plasma edge where $d\rho/dr$ often is large. Here we give a brief account of these properties of GAMs, including a discussion of the perturbed magnetic field in the vacuum region, and refer to [5] for a detailed analysis.

Main structure of the GAM field The analysis in [5] is based on a straight field line coordinate system (r, θ, φ) in which $\boldsymbol{\xi}$ and $\mathbf{Q}$ are represented by their contravariant components, i.e. $\boldsymbol{\xi} = \xi^r \mathbf{e}_r + \xi^\theta \mathbf{e}_\theta + \xi^\varphi \mathbf{e}_\varphi$ and $\mathbf{Q} = Q^r \mathbf{e}_r + Q^\theta \mathbf{e}_\theta + Q^\varphi \mathbf{e}_\varphi$. For a tokamak with large aspect ratio, $\boldsymbol{\xi}$ and Q^φ, including the leading-order $m = 2$ components, are given by the expansions

$$\xi^r = \varepsilon^2 \xi_2^{r(2)} \sin 2\theta + \cdots \tag{1a}$$
$$\xi^\theta = \xi_0^{\theta(0)} + \varepsilon \xi_1^{\theta(1)} \cos \theta + \varepsilon^2 \xi_2^{\theta(2)} \cos 2\theta + \cdots \tag{1b}$$
$$\xi^\varphi = \varepsilon \xi_1^{\varphi(1)} \cos \theta + \varepsilon^2 \xi_0^{\varphi(2)} + \varepsilon^2 \xi_2^{\varphi(2)} \cos 2\theta + \cdots \tag{1c}$$
$$Q^\varphi = \varepsilon^4 Q_1^{\varphi(4)} \sin \theta + \varepsilon^5 Q_2^{\varphi(5)} \sin 2\theta + \cdots \tag{1d}$$

The other two components of **Q** are given by the expansions $Q^r = \varepsilon^3 Q_2^{r(3)} \cos 2\theta + \cdots$ and $Q^\theta = \varepsilon^3 Q_2^{\theta(3)} \sin 2\theta + \cdots$, and the amplitudes $Q_2^{\theta(3)}$ and $Q_2^{r(3)}$ can, from $\mathbf{Q} = \nabla \times (\boldsymbol{\xi} \times \mathbf{B})$, be expressed directly in terms of $\xi_2^{r(2)}$ in (1a) as $Q_2^{\theta(3)} = -(B_0/rR_0)\left(r\mu\xi_2^{r(2)}\right)'$ and $Q_2^{r(3)} = (2\mu B_0/R_0)\xi_2^{r(2)}$, where $\mu \equiv 1/q$, B_0 is the toroidal magnetic field and R_0 the major radius of the plasma. For a perturbation $(\boldsymbol{\xi}, \mathbf{Q}) \sim e^{-i\omega t}$, a solution of the MHD equation of motion

yields, to leading order, the GAM components $\xi_0^{\theta(0)} = a\hat{\xi}\delta(r - r_0)$, $\xi_1^{\theta(1)} = \mu^2(r/R_0)\xi_0^{\theta(0)}$, $\xi_1^{\varphi(1)} = \mu(r/R_0)\xi_0^{\theta(0)}$ and $Q_1^{\varphi(4)} = -(r\Gamma p/B_0 R_0^2)(2 + \mu^2)\xi_0^{\theta(0)}$, where r_0 is a radius where $\omega^2 = \omega_{GAM}^2 = \omega_s^2(2 + \mu^2)$, and $\hat{\xi}$ is an arbitrary amplitude constant [4, 5]. Furthermore, $\omega_s = \sqrt{\Gamma p/\rho}/R_0$ is the sound frequency, p the plasma pressure, ρ the density and Γ the adiabatic index. The GAM components to next order in ε can be derived from $\xi_2^{r(2)}$ in (1a), which is obtained by solving the differential equation and boundary condition [5]

$$\frac{d}{dr}\left(\mu^2 r^3 \frac{d\xi_2^{r(2)}}{dr}\right) - 3\mu^2 r\xi_2^{r(2)} + \frac{r^3 R_0^2}{2B_0}\frac{d}{dr}\left(\frac{Q_1^{\varphi(4)}}{r}\right) = 0 \tag{2a}$$

$$a\frac{d\xi_2^{r(2)}}{dr}\bigg|_{r=a} = -\frac{1+3\lambda}{1-\lambda}\xi_2^{r(2)}(a) \tag{2b}$$

respectively, where a is the plasma radius, b $(> a)$ the radius of a surrounding, conducting wall, and $\lambda = (a/b)^4 < 1$. The boundary condition (2b) is obtained by matching the internal GAM field to the perturbed magnetic field in the vacuum region. Of the rest of the $m = 2$ components in (1b, c, d), $\xi_2^{\varphi(2)}$ exists only at the GAM surface while $\xi_2^{\theta(2)}$ and $Q_2^{\varphi(5)}$ in addition have parts that exist outside $r = r_0$. For instance, $\xi_2^{\theta(2)}\big|_{r\neq r_0} = \frac{1}{2}\left(d\xi_2^{r(2)}/dr + \xi_2^{r(2)}/r\right)$.

Magnetic components in the vacuum region By continuity of the structure of the r- and θ-components of **Q** across the plasma-vacuum interface, these components of the perturbed vacuum magnetic field have the form $\delta B_r(r)\cos 2\theta$ and $\delta B_\theta(r)\sin 2\theta$. It is easy to show that $\delta B_{r,\theta}$ both satisfy the equation $r^2(\delta B_{r,\theta})'' + 3r(\delta B_{r,\theta})' - 3\delta B_{r,\theta} = 0$ to leading order. The solution to this equation that fulfills $\delta B_r = 0$ at the conducting wall $r = b$ is given by

$$\delta B_{r,\theta}(r) = \frac{a\delta B_r(a)}{r}\left[\frac{1}{1-\lambda}\left(\frac{a}{r}\right)^2 \pm \frac{\lambda}{1-\lambda}\left(\frac{r}{a}\right)^2\right] \tag{3}$$

where the minus sign is valid for δB_r and the plus sign for δB_θ. From continuity of the radial component of **Q** it follows that $\delta B_r(a) = (2B_0/q_a R_0)\xi_2^{r(2)}(a)$, and based on the properties of the solution to (2a, b), $\delta B_{r,\theta}(a)/B_0$ can be expressed in the form $\varepsilon_a\beta^*(r_0)f_q(r_0)g_\pm\hat{\xi}$ where $\beta^*(r_0) = \omega_s^2/\omega_A^2$ is the beta value at the GAM surface, $f_q(r_0)$ a factor that depends on the q-profile and strongly on the GAM radius r_0, and $g_\pm$ are factors that depend mainly on the wall distance and rather weakly on the q-profile ($\delta B_r \propto g_-$ and $\delta B_\theta \propto g_+$) [5].

In Fig. 1a, $\delta B_r(r)/\delta B_r(a)$ (solid curves) and $\delta B_\theta(r)/\delta B_r(a)$ (dotted curves) given by (3) are shown for $b/a = 1.25$, 1.5, and 2. It is seen that δB_θ is significantly larger than δB_r in the vacuum region if there is a conducting wall close to the plasma, while the two components are of comparable magnitude if the wall is far from the plasma. In Fig. 1b, an example of a solution $\xi_2^{r(2)}(r)$ to (2a, b) is shown together with the associated magnetic components inside and outside a plasma with q-profile $q(r) = 1 + 3(r/a)^4$ and wall distance $b/a = 1.25$. Furthermore, $\beta^*(r_0) = 1$, $\hat{\xi} = 1$ and the GAM radius is $r_0 = 0.7a$.
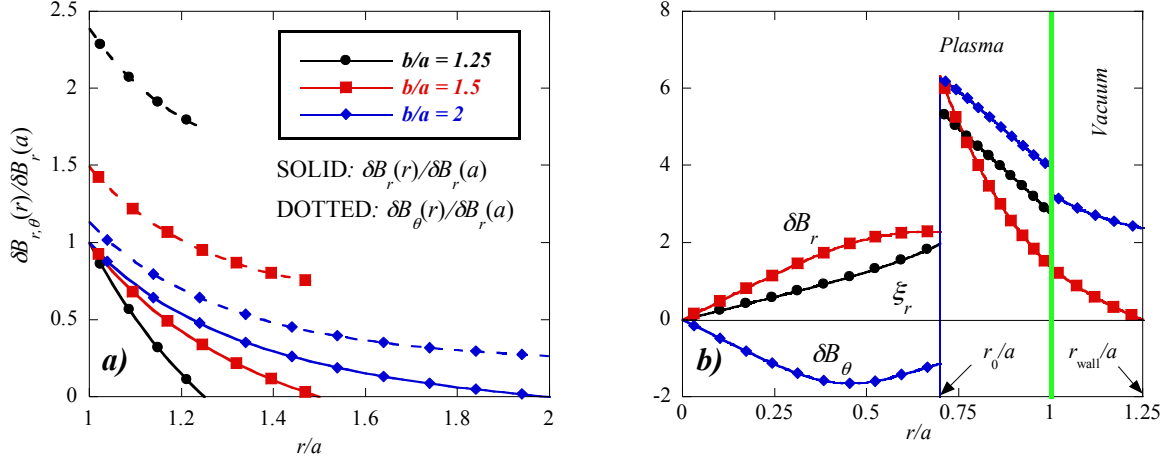
Fig. 1a) Normalized magnitudes of the magnetic components $\delta B_r(r)\cos 2\theta$ and $\delta B_\theta(r)\sin 2\theta$ in the vacuum region between the plasma surface and a conducting wall, for different wall distances b/a.
Fig. 1b) Plasma perturbation and magnetic components both inside and outside the plasma ($r_0 = r_{GAM}$).

In Fig. 2a, the combination of the factors $\beta^*(r_0)$ and $f_q(r_0)$ is shown for the two pressure profiles $\beta^*(r) = \beta^*(0)[1 - (r/a)^2]^\nu$ with $\nu = 1$ and 2, $\beta^*(0) = 1$, and for the q-profiles $q(r) = 1 + 5(r/a)^\alpha$ with $\alpha = 2, 4, 6$. It is seen that $\delta B_{vac}/B_0$ is maximized for GAMs localized relatively close to the plasma edge, with optimal values occurring for $r_0/a \sim 0.7 - 0.9$, depending a little on the pressure and q-profiles. Fig. 2b illustrates $g_\pm(b/a)$ for the same q-profiles as in Fig. 2a. For b/a near unity, δB_θ is seen to be much larger than δB_r ($g_+ \gg g_-$).
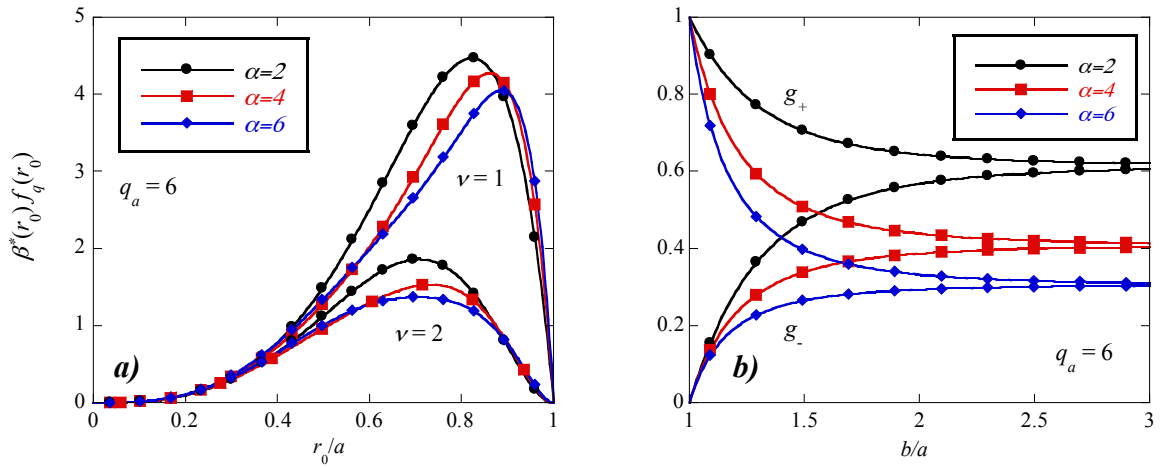

Fig. 2a) Product of $\beta^*(r_0)$ and $f_q(r_0)$ determining $\delta B_{r,\theta}(a)$. The pressure profile is $\beta^*(0)[1 - (r/a)^2]^\nu$ with $\beta^*(0) = 1$, $\nu = 1$ and 2, and the q-profiles are given by $q(r) = 1 + (q_a - 1)(r/a)^\alpha$ with $\alpha = 2, 4, 6$ and $q_a = 6$. Fig. 2b) Magnitude of the factors $g_\pm(b/a)$ determining the effect of the conducting wall on $\delta B_{r,\theta}(a)$. ($\delta B_r \propto g_-$ and $\delta B_\theta \propto g_+$). The q-profiles are the same as in (a).

Global $m = 2$ components In addition to the global structure of the $m = 2$ components of $\xi^{r,\theta}$ and $\delta B_{r,\theta}$, the GAM field also includes global pressure and density perturbations [5]. The global density perturbation, for instance, is given by $\delta\rho|_{r\neq r_0} = -\xi_2^{r(2)}(d\rho/dr)\sin 2\theta$ and is generated by a finite $\xi_2^{r(2)}$. A realistic estimate of these fluctuations requires that $\xi_2^{r(2)}$ is solved with a free plasma boundary together with the boundary condition (2b). Examples of the type of global $m = 2$ fluctuations in ξ^θ and ρ that the solutions to (2a, b) generate are shown in Fig. 3.
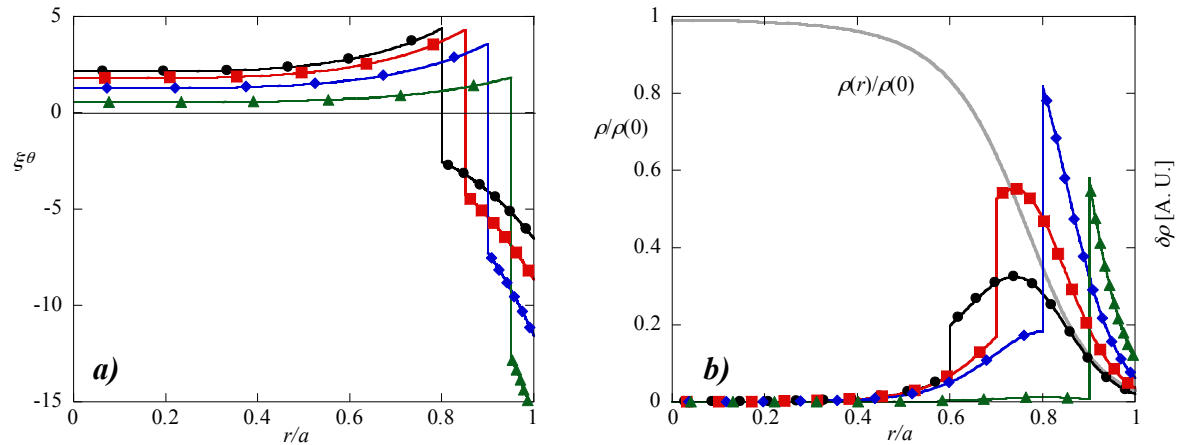
Fig. 3a) Amplitude of global $m = 2$ oscillations of the poloidal flow associated with GAMs localized at $r_0/a = 0.8, 0.85, 0.9$ and 0.95. Fig 3b) Perturbed density $\delta\rho$ outside the GAM surface produced by GAMs localized at $r_0/a = 0.6, 0.7, 0.8$ and 0.9 in the density profile shown. $\hat{\xi} = 1$, $\beta^*(r_0) = 1$ and the q-profile is $q(r) = 1 + 3(r/a)^4$ in both figures. The wall distance is $b/a = 1.25$ in (a) and 1.15 in (b).

Typically, these fluctuations tend to be strongest on the outside of the GAM surface $r = r_0$, and especially in the edge region of the plasma, as seen in Fig. 3a. Furthermore, as shown in Fig. 3b, the fluctuations in ρ are particularly strong in regions where the density gradient is large, somewhat similar to the measured GAM intensities e.g. in [6].

Conclusions A detailed MHD analysis [5] of axisymmetric ($m = n = 0$) modes in tokamaks with large aspect ratio and circular cross section leads to results consistent with the experimentally observed main structure of the perturbed vacuum magnetic field associated with GAMs [2, 3]. Furthermore, although these GAM solutions belong to the MHD continuum, the associated $m = 2$ perturbations at the same frequency in magnetic field, plasma flow, plasma density and plasma pressure nevertheless have such an extension across the plasma and vacuum regions (see e.g. Figs. 1b and 3a, b) that they are in essence "global modes". It is therefore not unlikely that the GAM eigenmode structures diagnosed in several recent experiments (e.g. [2] and [7]) could be the result of the radially extended $m = 2$ components (plus additional harmonics in plasmas with a non-circular cross section [5]) of the perturbed density and poloidal flow of a single continuum mode localized near the plasma edge.

Acknowlededments

References
[1]   N Winsor, J L Johnson and J M Dawson, Phys. Fluids **11**, 2448,1968.
[2]   C A de Meijere *et al* Plasma Phys. Control. Fusion **56**, 072001, 2014.
[3]   V V Bulanin *et al* Nucl. Fusion **56**, 016017, 2016.
[4]   C Wahlberg, Phys. Rev. Lett. **101**, 115003, 2008; Plasma Phys. Control. Fusion **51**, 085006, 2009.
[5]   C Wahlberg and J P Graves, Plasma Phys. Control. Fusion **58**, 075014, 2016.
[6]   G D Conway *et al* Plasma Phys. Control. Fusion **50**, 055009, 2008; C Silva *et al* Plasma Phys. Control. Fusion **55**, 025001, 2013.
[7]   A V Melnikov *et al* Nucl. Fusion **55**, 063001, 2015.